TOKYO J. MATH.
VOL. 26, NO. 1, 2003

Classification of Spatial Polygons that Could Possibly Generate Embedded Triply Periodic Minimal Surfaces

Tetsuro KAWASAKI

Gakushuin University

1. Introduction

A regular tetrahedron has six edges. Choose a pair of non-adjacent edges. Then the other four edges form a spatial quadrilateral. In about 1865, H. A. Schwarz and B. Riemann independently constructed a solution of Plateau's problem for this contour. It is called the Riemann-Schwarz' diamond surface.

In general a minimal surface can be continued analytically by the line symmetry of a line segment of its boundary. By repeated applications of this process to the Riemann-Schwarz' diamond surface, we get a triply periodic minimal surface. We express all these processes as "the skew quadrilateral generates a triply periodic minimal surface".

A spatial polygon is a simple closed curve in $\mathbf{R}^3$ consisting of a finite number of edges. We say that a spatial polygon Γ **generates** a triply periodic minimal surface S if

i) S contains a compact domain S_Γ bounded by Γ, and

ii) let G be the congruence group generated by the rotation of angle π about the lines containing the edges of Γ, then

$$S = \bigcup_{g \in G} g\, S_\Gamma .$$

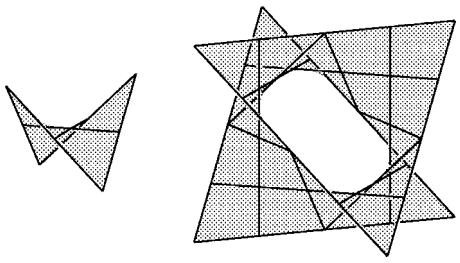

FIGURE 1. The Riemann-Schwarz' diamond surface and its continuation.

Received August 7, 2001; revised December 1, 2001

In this paper, we classify spatial polygons that could possibly generate embedded triply periodic minimal surfaces. There are 21 types of such spatial polygons. They are listed in terms of crystallographic groups. The line symmetries of the edges of such a polygon generate a crystallographic group. The crystallographic groups are partitioned into the seven crystal systems, by the types of lattices that they contain. They are triclinic, monoclinic, orthorhombic, tetragonal, trigonal, hexagonal and cubic crystal systems. Since our crystallographic group is generated by line symmetries, the possible crystal system is orthorhombic, tetragonal, trigonal, hexagonal or cubic crystal system.

There are five types of spatial polygons that could possibly generate embedded triply periodic minimal surfaces whose crystallographic groups belong to orthorhombic crystal system, that is, with a lattice of rectangular parallelepiped.

There are four types of spatial polygons that could possibly generate embedded triply periodic minimal surfaces whose crystallographic groups belong to tetrahedral crystal system, that is, with a lattice of right square cylinder.

There is no spatial polygon that generate embedded triply periodic minimal surfaces whose crystallographic groups belong to trigonal crystal system.

There are only two types of spatial polygons that could possibly generate embedded triply periodic minimal surfaces whose crystallographic groups belong to hexagonal crystal system, that is, with a lattice of right, regular hexagonal cylinder.

There are ten types of spatial polygons that could possibly generate embedded triply periodic minimal surfaces whose crystallographic groups belong to cubic crystal system, that is, with a cubic lattice.

We restate our result in the form of a theorem.

THEOREM. *Let S be an embedded triply periodic minimal surface generated by a spa-*

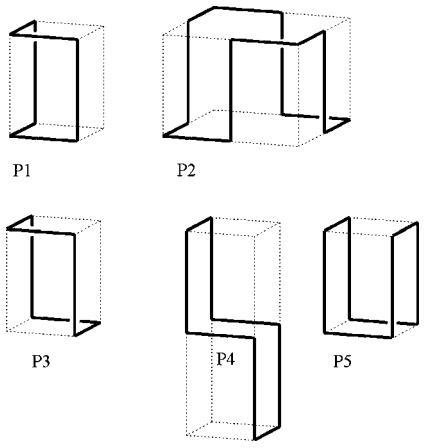

FIGURE 2. Spatial polygons with orthorhombic lattices.

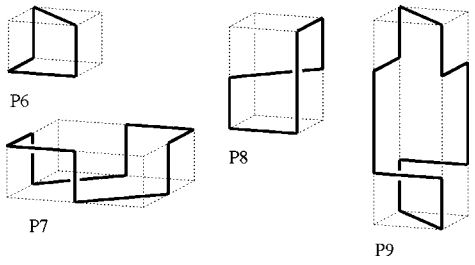

FIGURE 3. Spatial polygons with tetrahedral lattices.

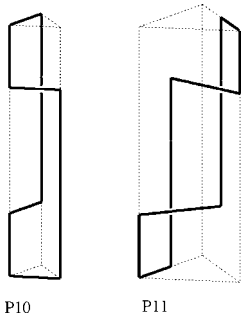

FIGURE 4. Spatial polygons with hexagonal lattices.

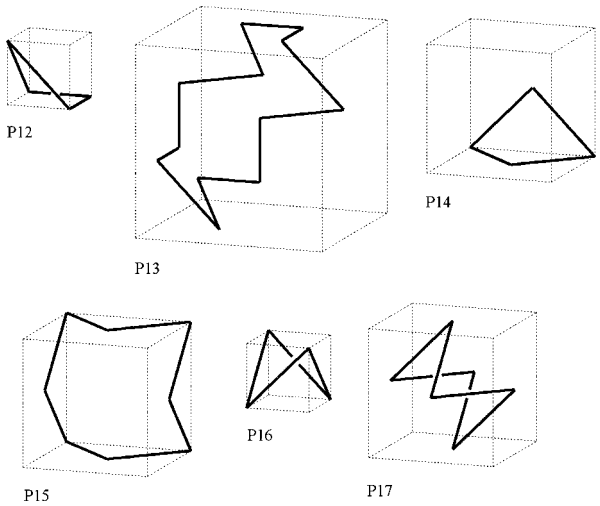

FIGURE 5. Spatial polygons with cubic lattices (I).

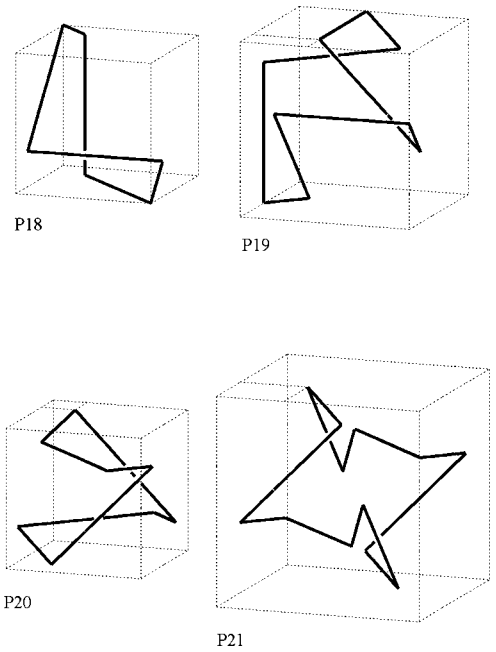

FIGURE 6. Spatial polygons with cubic lattices (II).

tial polygon Γ. Then Γ belongs to one of 21 *types*: P1–P21.

REMARK. Here, we do not discuss the existence of bounding minimal surfaces of Γ. We assume the existence of the embedded triply periodic minimal surface S, generated by a spatial polygon Γ. Let S_Γ be a part of S bounded by Γ. We do not assume S_Γ to be simply-connected. We only assume that S_Γ is a compact minimal surface with boundary Γ. The crucial assumption is the embeddedness. This assumption is effective to reduce the types of spatial polygons. Many of these polygons are known to generate embedded triply periodic minimal surfaces [1, 5, 9]. We will refer to them later, see Section 5.

The proof of this theorem consists of two stages. In the first stage, we list up all the possible configurations contained in triply periodic minimal surfaces. There are 36 types of such configurations. Then, as the second stage, we search the possibility of finding spatial polygons. Among 36 configurations, only 12 contain generating spatial polygons.

The author wishes to express his thanks to the referee who helped him to complete Section 5.

2. Crystallographic groups generated by line symmetries

Let G be a crystallographic group and let T be its lattice subgroup, that is, G is a discrete group of isometries of $\mathbf{R}^3$ and T is the subgroup of G consisting of all the translations. The translation vectors of T form a lattice in $\mathbf{R}^3$. Then T is a normal subgroup of G and the quotient group $\lambda G = G/T$ is a finite subgroup in $O(3)$. This subgroup λG is called the point group of G. The conjugacy class of a point group is called the crystal class. It is well-known that there are only 32 crystal classes.

Now we assume that G is generated by line symmetries. Then λG is generated by line symmetries of at least two independent directions. So λG is a subgroup of $SO(3)$ and its crystal class is one of five crystal classes:

$$D_2,\ D_4,\ D_3,\ D_6,\ O\ ,$$

that is, the dihedral group of order 4, 8, 6 or 12, or the octahedral group of order 24. Its crystal system is orthorhombic, tetragonal, trigonal, hexagonal, or cubic, respectively.

2.1. Orthorhombic system D_2. The group D_2 is generated by line symmetries of x-, y- and z-axes. There are nine crystallographic groups in the crystal class D_2, among which five groups are generated by line symmetries:

$$P222,\ P222_1,\ C222,\ F222,\ I2_12_12_1\ .$$

2.2. Tetragonal system D_4. The group D_4 is generated by line symmetries of x- and 110-axes. It also contains the rotation of order 4 around z-axis. There are eight crystallographic groups in the crystal class D_4, among which five groups are generated by line symmetries:

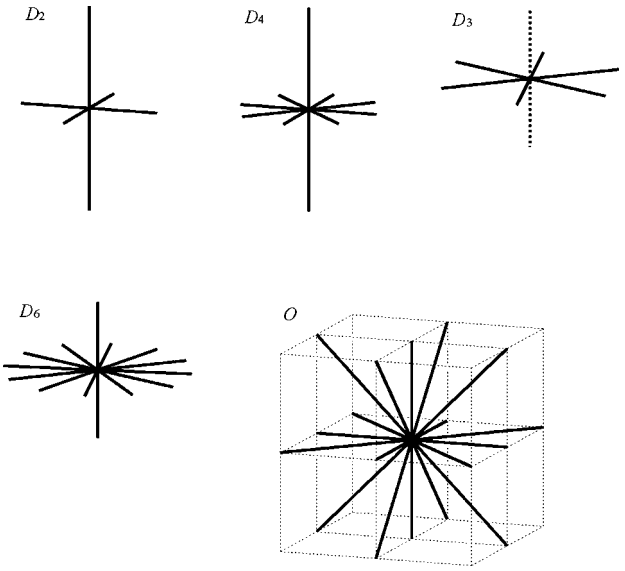

FIGURE 7. Point groups D_2, D_4, D_3, D_6, O.

$$P422,\ P4_122,\ P4_222,\ I422,\ I4_122\,.$$

2.3. Trigonal system D_3. The group D_3 is generated by line symmetries of x- and $\frac{\pi}{3}$-axes, here θ-axis means the ray in xy-plane, with angle θ from x-axis. It also contains the rotation of order 3 around z-axis. There are five crystallographic groups in the crystal class D_3, among which three groups are generated by line symmetries:

$$P312,\ P3_112,\ R32\,.$$

2.4. Hexagonal system D_6. The group D_6 is generated by line symmetries of x- and $\frac{\pi}{6}$-axes. It also contains the rotation of order 6 around z-axis. There are four crystallographic groups in the crystal class D_6, all of which are generated by line symmetries:

$$P622,\ P6_122,\ P6_222,\ P6_322\,.$$

2.5. Cubic system O. The group O is generated by line symmetries of x-, 110- and 101-axes. It also contains the rotation of order 4 around z-axis, and also the rotation of order 3 around 111-axis. There are seven crystallographic groups in the crystal class O, all of which are generated by line symmetries:

$$P432,\ P4_232,\ F432,\ F4_132,\ I432,\ P4_332,\ I4_132\,.$$

3. Configurations of triply periodic minimal surfaces

Let S be a complete, triply periodic minimal surface embedded in the Euclidean space $\mathbf{R}^3$ and let $\mathcal{L}$ be the set of all lines contained in S. We assume that $\mathcal{L}$ is so large that the symmetries of $\mathcal{L}$ generate a crystallographic group G. This is equivalent to the condition that S contains at least two non-parallel lines. We call $\mathcal{L}$ the **configuration** of S. Since S is stable under the symmetry of a line in S, G is a subgroup of the congruent transformation group of S.

Now G is one of the crystallographic groups listed in the previous section. Let $\tilde{\mathcal{L}}$ be the axes of the line symmetries (π-rotations) in G. Then, $\mathcal{L}$ is a subet of $\tilde{\mathcal{L}}$. Since $\mathcal{L}$ is invariant by the actions of G, it is a union of G-orbits in $\tilde{\mathcal{L}}$.

We call x to be a **vertex** of the configuration $\mathcal{L}$, if it is an intersection point of lines in $\tilde{\mathcal{L}}$. We denote the isotropy subgroup at x by G_x, the lines through x by $\mathcal{L}_x = \{l \in \mathcal{L} \mid x \in l\}$ and by $\tilde{\mathcal{L}}_x = \{l \in \tilde{\mathcal{L}} \mid x \in l\}$. Since G_x does not contain translations, we can consider G_x as a subgroup of λG. So, it is conjugate to D_2, D_4, D_3, D_6 or O. We call this conjugacy class as the type of a vertex x. We can exclude the possibility of type O.

We denote the tangent plane of S at x by Π_x. It is invariant by the action of G_x. Also, we have $\mathcal{L}_x = \{l \in \tilde{\mathcal{L}}_x \mid l \subset \Pi_x\}$. If there exists $l \in \tilde{\mathcal{L}}_x \setminus \mathcal{L}_x$, then Π_x is invariant by the symmetry of l and $l \not\subset \Pi_x$, or we have $l = \Pi_x^{\perp}$. Therefore, either $\tilde{\mathcal{L}}_x = \mathcal{L}_x$ or $\tilde{\mathcal{L}}_x = \mathcal{L}_x \cup \{\Pi_x^{\perp}\}$.

For a vertex of type O, we cannot find such a decomposition. So, there are no vertices of type O. For vertices of type D_4, D_3 or D_6, $\mathcal{L}_x$ is uniquely determined by $\tilde{\mathcal{L}}_x$. As for a vertex of type D_2, there are three possibilities of $\mathcal{L}_x$, for each given $\tilde{\mathcal{L}}_x$.

3.1. Orthorhombic system D_2

3.1.1. $P222$

$\tilde{\mathcal{L}}$ consists of twelve G-orbits. We name $\alpha_1, \alpha_2, \alpha_3, \alpha_4$ the orbits parallel to x-axis, $\beta_1, \beta_2, \beta_3, \beta_4$ the orbits parallel to y-axis and $\gamma_1, \gamma_2, \gamma_3, \gamma_4$ the orbits parallel to z-axis. All the vertices of $\tilde{\mathcal{L}}$ are of type D_2. Then, for each vertex, $\mathcal{L}$ selects two lines out of three lines of $\tilde{\mathcal{L}}$. Therefore, for each small rectangular parallelepiped, the edges of $\mathcal{L}$ gives a simple closed curves, or their disjoint union. We get five patterns. One does not generate G. Each of the other four generate G. Thus we get four possible configurations. See Figs. 9, 10.

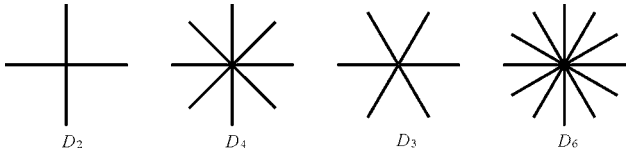

FIGURE 8. Vertices of type D_2, D_4, D_3, D_6.

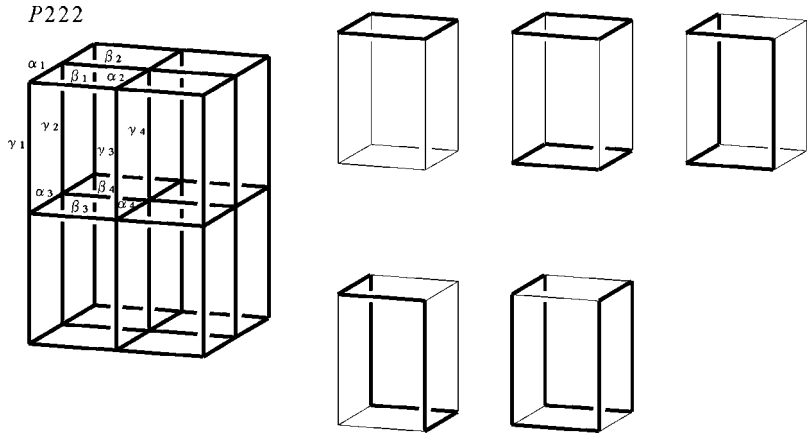

FIGURE 9. $P222$, G-orbits and simple closed curves.

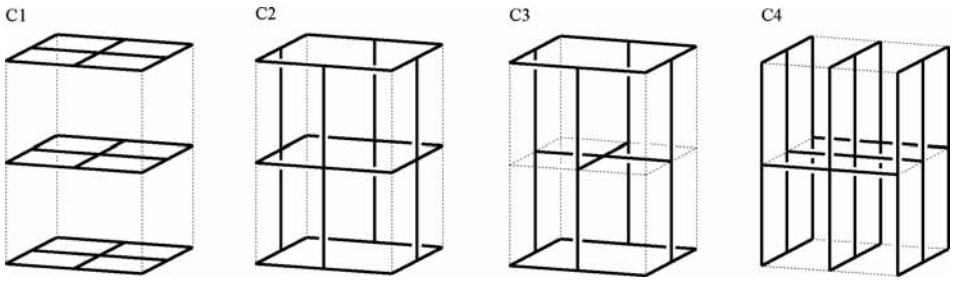

FIGURE 10. Configurations: C1 $\sim$ C4.

C1: $\mathcal{L} = \alpha_1 \cup \alpha_2 \cup \alpha_3 \cup \alpha_4 \cup \beta_1 \cup \beta_2 \cup \beta_3 \cup \beta_4$
C2: $\mathcal{L} = \alpha_1 \cup \alpha_3 \cup \beta_1 \cup \beta_3 \cup \gamma_2 \cup \gamma_3$
C3: $\mathcal{L} = \alpha_1 \cup \alpha_4 \cup \beta_1 \cup \beta_4 \cup \gamma_2 \cup \gamma_3$
C4: $\mathcal{L} = \alpha_1 \cup \alpha_2 \cup \beta_3 \cup \beta_4 \cup \gamma_1 \cup \gamma_2 \cup \gamma_3 \cup \gamma_4$

3.1.2. $P222_1$

$\tilde{\mathcal{L}}$ consists of four G-orbits. We name α_1, α_2 the orbits parallel to x-axis and β_1, β_2 the orbits parallel to y-axis. We need all four G-orbits to generate G. Thus $\mathcal{L} = \tilde{\mathcal{L}}$. See Fig. 11.

C5: $\mathcal{L} = \tilde{\mathcal{L}} = \alpha_1 \cup \alpha_2 \cup \beta_1 \cup \beta_2$

3.1.3. $C222$

$\tilde{\mathcal{L}}$ consists of seven G-orbits. We name α_1, α_2 the orbits parallel to x-axis, β_1, β_2 the orbits parallel to y-axis and $\gamma_1, \gamma_2, \gamma_3$ the orbits parallel to z-axis. Without γ_3 orbit, other orbits do not generate G. For the other six orbits, the same situation happens as the case

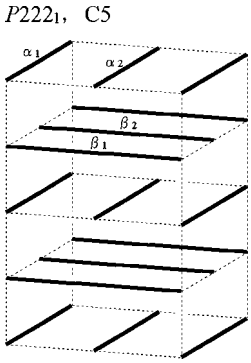

FIGURE 11. $P222_1$, G-orbits, configurations: C_5.

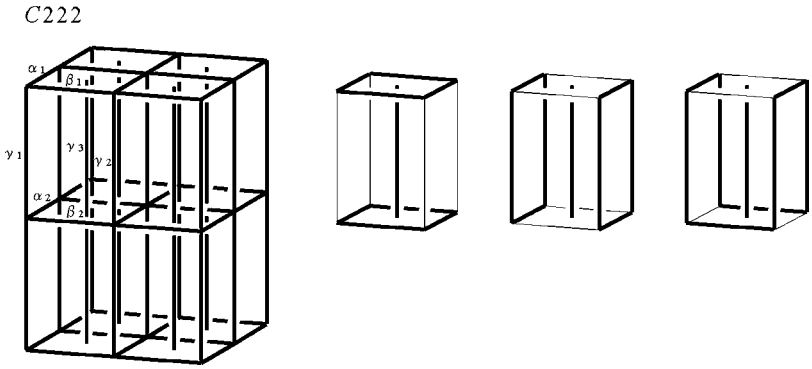

FIGURE 12. $C222$, G-orbits, simple closed curves.

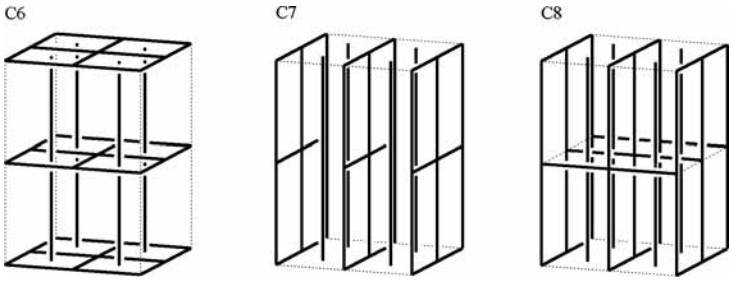

FIGURE 13. Configurations: C6 $\sim$ C8.

$P222$. Because $\mathcal{L}$ is symmetric with respect to γ_3, only two patterns are possible. See Figs. 12, 13.

C6: $\mathcal{L} = \alpha_1 \cup \alpha_2 \cup \beta_1 \cup \beta_2 \cup \gamma_3$
C7: $\mathcal{L} = \alpha_1 \cup \alpha_2 \cup \gamma_1 \cup \gamma_2 \cup \gamma_3$
C8: $\mathcal{L} = \alpha_1 \cup \beta_2 \cup \gamma_1 \cup \gamma_2 \cup \gamma_3$

3.1.4. $F222$

$\tilde{\mathcal{L}}$ consists of six G-orbits. We name α_1, α_2 the orbits parallel to x-axis, β_1, β_2 the orbits parallel to y-axis and γ_1, γ_2 the orbits parallel to z-axis. For each i, $i = 1, 2$, α_i, β_i and γ_i meet at a vertex. So, we have to choose two out of three. By the symmetry, we get two configurations. See Fig. 14.

C9: $\mathcal{L} = \alpha_1 \cup \alpha_2 \cup \beta_1 \cup \beta_2$
C10: $\mathcal{L} = \alpha_1 \cup \alpha_2 \cup \beta_1 \cup \gamma_2$

3.1.5. $I2_12_12_1$

$\tilde{\mathcal{L}}$ consists of three G-orbits. We name α the orbit parallel to x-axis, β the orbit parallel to y-axis and γ the orbit parallel to z-axis. We need all three G-orbits to generate G. Thus $\mathcal{L} = \tilde{\mathcal{L}}$. See Fig. 15.

C11: $\mathcal{L} = \tilde{\mathcal{L}} = \alpha \cup \beta \cup \gamma$

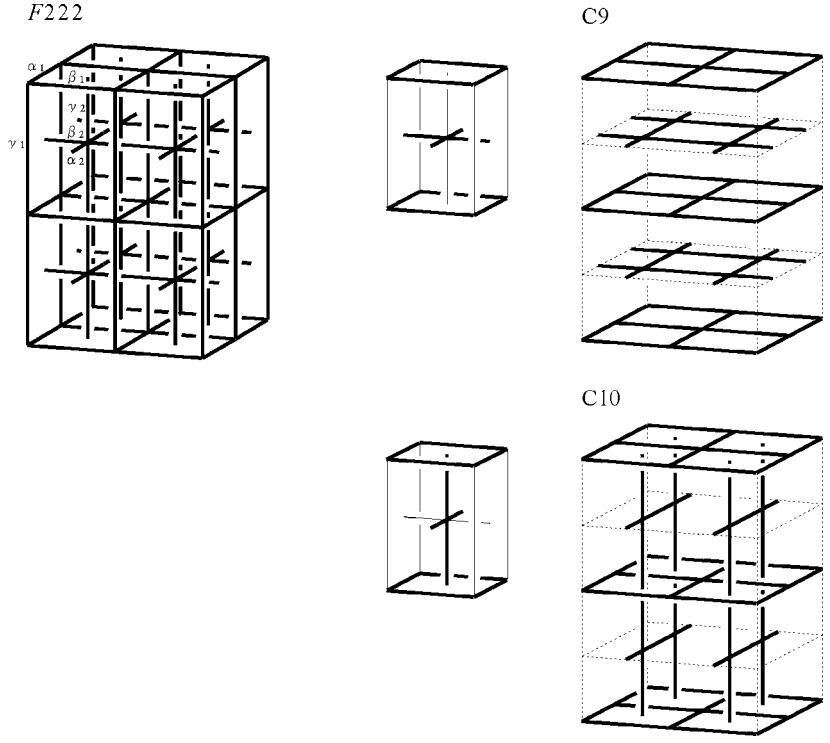

FIGURE 14. $F222$, G-orbits, configurations: C9, C10.

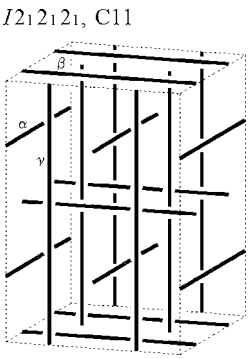

FIGURE 15. $I2_12_12_1$, G-orbits, configuration: C11.

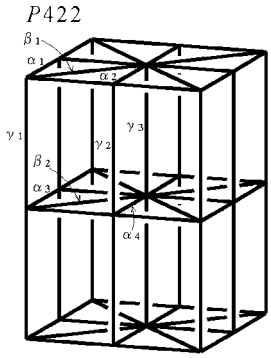

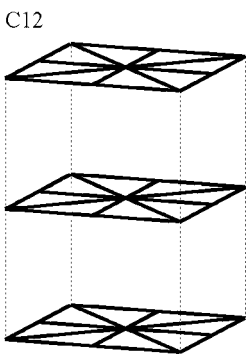

FIGURE 16. $P422$, G-orbits, configuration: C12.

3.2. Tetragonal system D_4

3.2.1. $P422$

$\tilde{\mathcal{L}}$ consists of nine G-orbits. We name $\alpha_1, \alpha_2, \alpha_3, \alpha_4$ the orbits parallel to x-axis, β_1, β_2 the orbits parallel to 110-axis and $\gamma_1, \gamma_2, \gamma_3$ the orbits parallel to z-axis. Because there exists a vertex of type D_4, if $\mathcal{L}$ contains one of α_1, α_2 or β_1, then it contains three, and so is for α_3, α_4 or β_2. Thus we get one possible configuration. See Fig. 16.

C12: $\mathcal{L} = \alpha_1 \cup \alpha_2 \cup \alpha_3 \cup \alpha_4 \cup \beta_1 \cup \beta_2$

3.2.2. $P4_122$

$\tilde{\mathcal{L}}$ consists of three G-orbits. We name α_1, α_2 the orbits parallel to x-axis and β the orbit parallel to 110-axis. We need all three G-orbits to generate G. Thus $\mathcal{L} = \tilde{\mathcal{L}}$. See Fig. 17.

C13: $\mathcal{L} = \tilde{\mathcal{L}} = \alpha_1 \cup \alpha_2 \cup \beta$

3.2.3. $P4_222$

$\tilde{\mathcal{L}}$ consists of nine G-orbits. We name $\alpha_1, \alpha_2, \alpha_3, \alpha_4$ the orbits parallel to x-axis, β_1, β_2 the orbits parallel to 110-axis and $\gamma_1, \gamma_2, \gamma_3$ the orbits parallel to z-axis. All the vertices are of type D_2. The intersecting triads are:

$$(\alpha_1, \alpha_3, \gamma_1),\ \ (\alpha_2, \alpha_3, \gamma_2),\ \ (\alpha_2, \alpha_4, \gamma_3),\ \ (\alpha_1, \alpha_4, \gamma_2),\ \ (\beta_1, \beta_2, \gamma_1),\ \ (\beta_1, \beta_2, \gamma_3)\,.$$

$\mathcal{L}$ must contain β_1 or β_2. By the symmetry, we may assume that $\mathcal{L}$ contains β_1. The choices of α's and γ's are the choices of simple closed curves in the parallelepiped. Thus we get four possible configurations. See Figs. 18, 19.

C14: $\mathcal{L} = \alpha_1 \cup \alpha_2 \cup \alpha_3 \cup \alpha_4 \cup \beta_1 \cup \beta_2$
C15: $\mathcal{L} = \alpha_1 \cup \alpha_3 \cup \beta_1 \cup \beta_2 \cup \gamma_2$
C16: $\mathcal{L} = \alpha_1 \cup \alpha_4 \cup \beta_1 \cup \gamma_1 \cup \gamma_3$

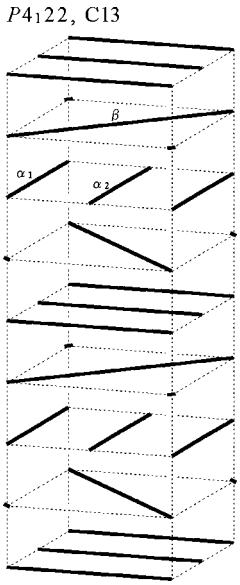

FIGURE 17. $P4_122$, G-orbits, configuration: C13.

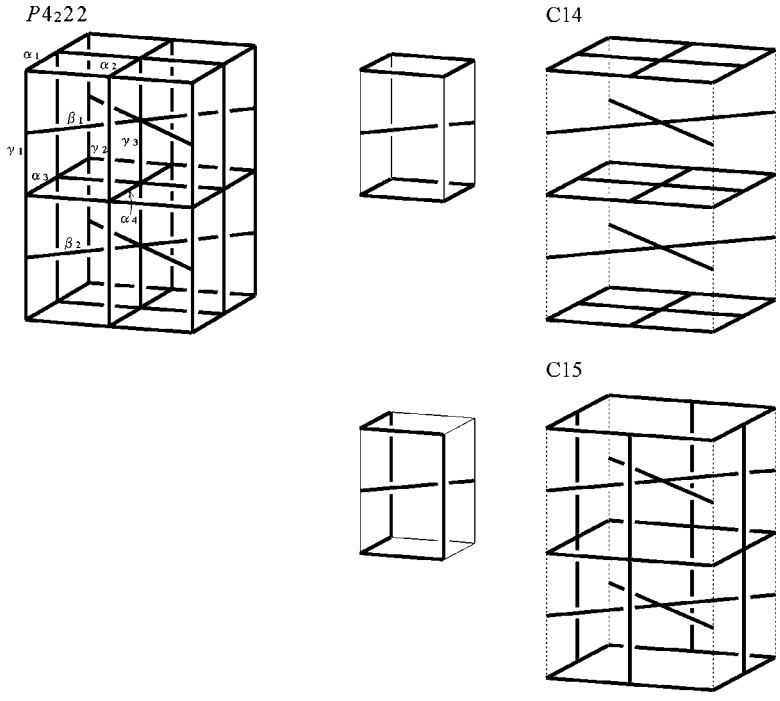

FIGURE 18. $P4_222$, G-orbits, configurations: C14, C15.

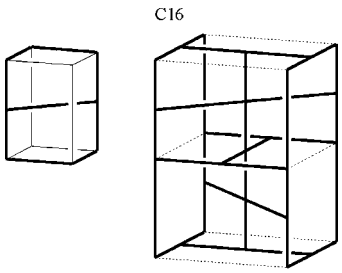

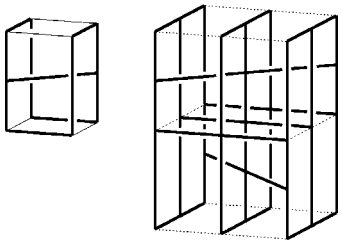

FIGURE 19. configurations: C16, C17.

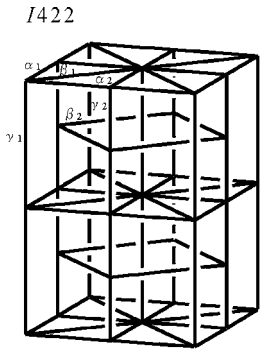

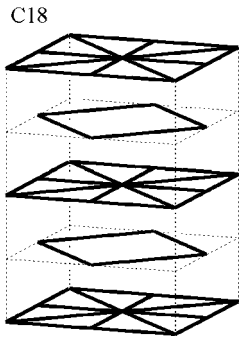

FIGURE 20. $I422$, G-orbits, configuration: C18.

C17: $\mathcal{L} = \alpha_1 \cup \alpha_2 \cup \beta_1 \cup \gamma_1 \cup \gamma_2 \cup \gamma_3$

3.2.4. $I422$

$\tilde{\mathcal{L}}$ consists of six G-orbits. We name α_1, α_2 the orbits parallel to x-axis, β_1, β_2 the orbits parallel to 110-axis and γ_1, γ_2 the orbits parallel to z-axis. Since there exists a vertex of type D_4, $\mathcal{L}$ does not contain γ's. To generate G we need all the other G-orbits. See Fig. 20.

C18: $\mathcal{L} = \alpha_1 \cup \alpha_2 \cup \beta_1 \cup \beta_2$

3.2.5. $I4_122$

$\tilde{\mathcal{L}}$ consists of four G-orbits. We name α the orbit parallel to x-axis, β_1, β_2 the orbits parallel to 110-axis and γ the orbit parallel to z-axis. There exists only one vertex of type D_2. We get two possible configurations. See Figs. 21, 22.

C19: $\mathcal{L} = \alpha \cup \beta_1 \cup \beta_2$
C20: $\mathcal{L} = \alpha \cup \beta_1 \cup \gamma$

$I4_122$

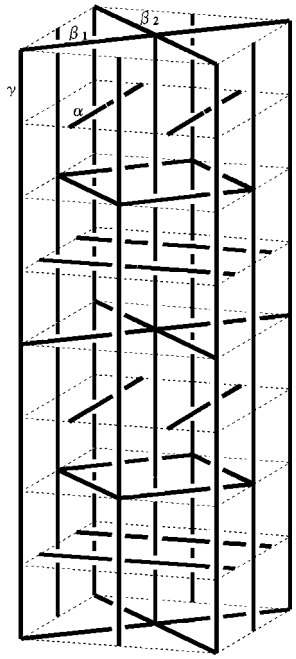

FIGURE 21. $I4_122$, G-orbits.

C19

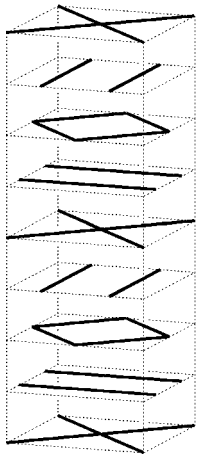

C20

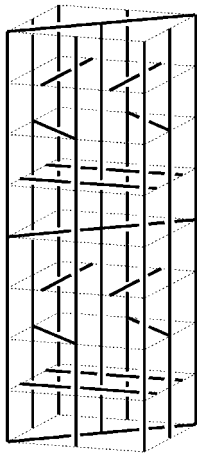

FIGURE 22. Configurations: C19, C20.

$P312$, C21

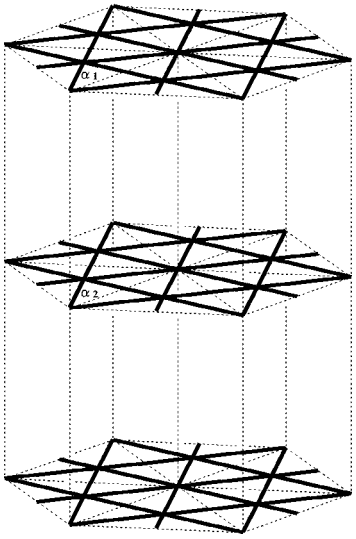

FIGURE 23. $P312$, G-orbits, configuration: C21.

$P3_112$, C22

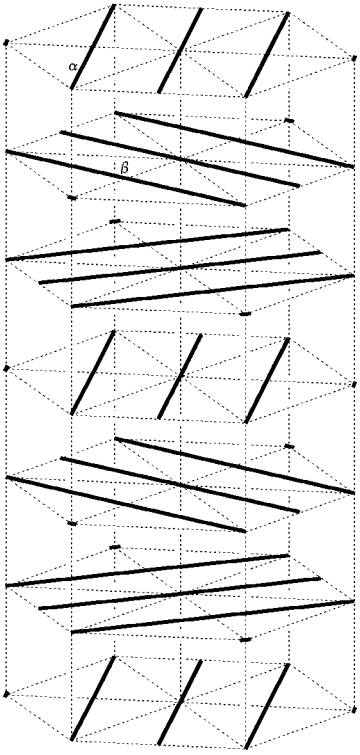

FIGURE 24. $P3_112$, G-orbits, configuration: C22.

$R32$, C23

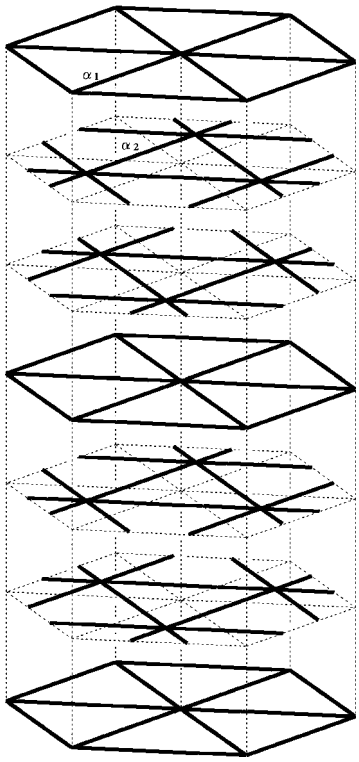

FIGURE 25. $R32$, G-orbits, configuration: C23.

3.3. Trigonal system D_3

3.3.1. $P312$

$\tilde{\mathcal{L}}$ consists of two G-orbits. We name α_1 the orbit on the top level and α_2 the orbit on the second level. Since we need both orbits to generate G, we have $\mathcal{L} = \tilde{\mathcal{L}}$. See Fig. 23.

C21: $\mathcal{L} = \tilde{\mathcal{L}} = \alpha_1 \cup \alpha_2$

3.3.2. $P3_112$

$\tilde{\mathcal{L}}$ consists of two G-orbits. We name α the orbit on the top level and β the orbit on the second level. Since we need both orbits to generate G, we have $\mathcal{L} = \tilde{\mathcal{L}}$. See Fig. 24.

C22: $\mathcal{L} = \tilde{\mathcal{L}} = \alpha \cup \beta$

3.3.3. $R32$

$\tilde{\mathcal{L}}$ consists of two G-orbits. We name α_1 the orbit on the top level and α_2 the orbit on the second level. Since we need both orbits to generate G, we have $\mathcal{L} = \tilde{\mathcal{L}}$. See Fig. 25.

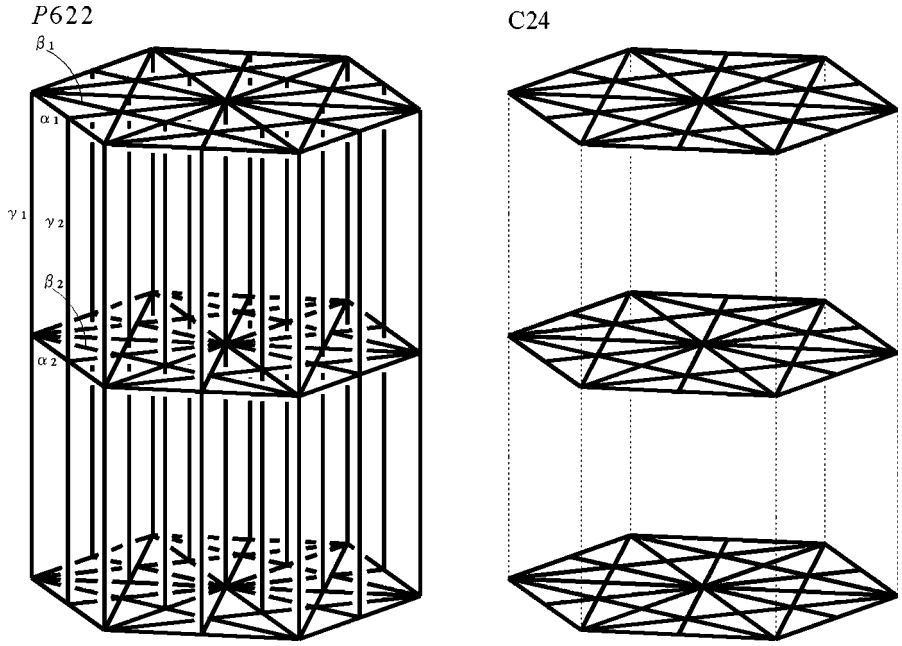

FIGURE 26. $P622$, G-orbits, configuration: C24.

C23: $\mathcal{L} = \tilde{\mathcal{L}} = \alpha_1 \cup \alpha_2$

3.4. Hexagonal system D_6

3.4.1. $P622$

$\tilde{\mathcal{L}}$ consists of six G-orbits. We name α_1, β_1 the orbits on the top level, α_2, β_2 the orbits on the second level and γ_1, γ_2 the orbits parallel to z-axis. Since there exists a vertex of type D_6, $\mathcal{L}$ contains α's and β's, and does not contain γ's. See Fig. 26.

C24: $\mathcal{L} = \alpha_1 \cup \alpha_2 \cup \beta_1 \cup \beta_2$

3.4.2. $P6_122$

$\tilde{\mathcal{L}}$ consists of two G-orbits. We name α the orbit on the top level and β the orbit on the second level. We need both orbits to generate G. See Fig. 27.

C25: $\mathcal{L} = \tilde{\mathcal{L}} = \alpha \cup \beta$

3.4.3. $P6_222$

$\tilde{\mathcal{L}}$ consists of six G-orbits. We name α_1, β_1 the orbits on the top level, α_2, β_2 the orbits on the second level and γ_1, γ_2 the orbits parallel to z-axis. All vertices are of type D_2. The intersecting triads are:

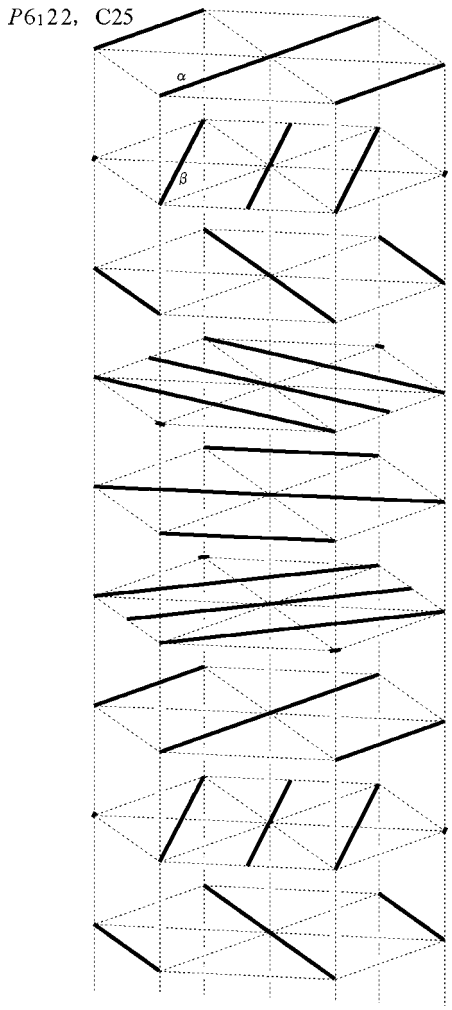

FIGURE 27. $P6_122$, G-orbits, configuration: C25.

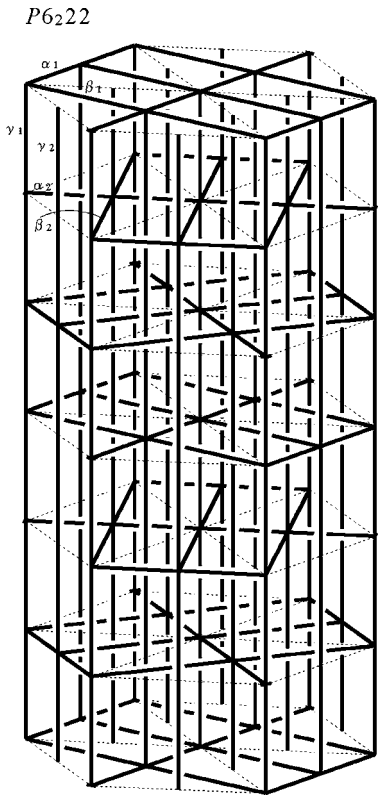

FIGURE 28. $P6_222$, G-orbits.

$$(\alpha_1, \beta_1, \gamma_1), \quad (\alpha_1, \beta_1, \gamma_2), \quad (\alpha_2, \beta_2, \gamma_1), \quad (\alpha_2, \beta_2, \gamma_2)\,.$$

We get four possible configurations. See Figs. 28, 29, 30.

C26: $\mathcal{L} = \alpha_1 \cup \alpha_2 \cup \beta_1 \cup \beta_2$
C27: $\mathcal{L} = \alpha_1 \cup \alpha_2 \cup \gamma_1 \cup \gamma_2$
C28: $\mathcal{L} = \beta_1 \cup \beta_2 \cup \gamma_1 \cup \gamma_2$
C29: $\mathcal{L} = \alpha_1 \cup \beta_2 \cup \gamma_1 \cup \gamma_2$

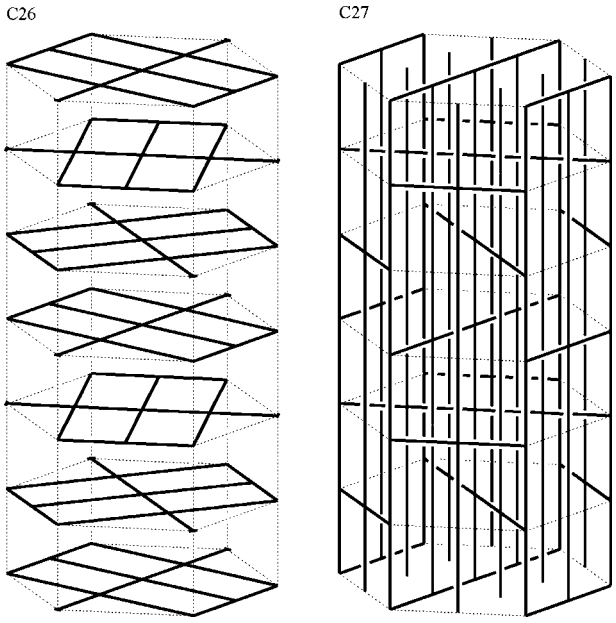

FIGURE 29. Configurations: C26, C27.

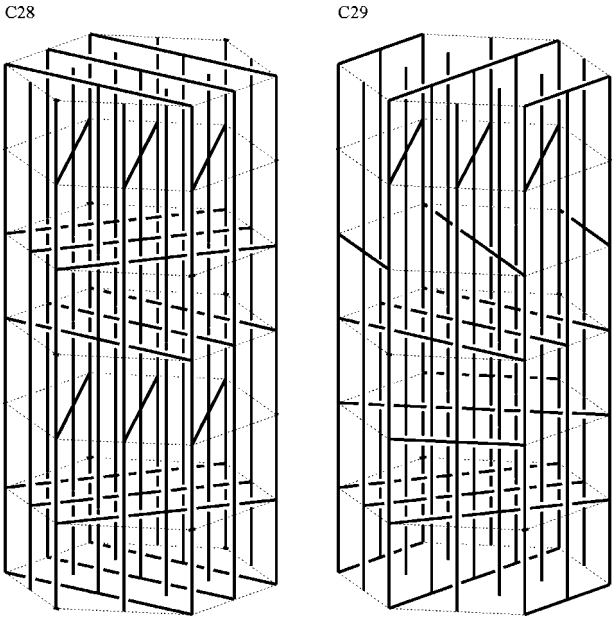

FIGURE 30. Configurations: C28, C29.

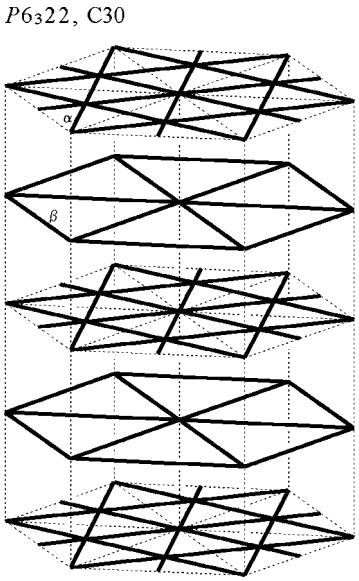

FIGURE 31. $P6_322$, G-orbits, configuration: C30.

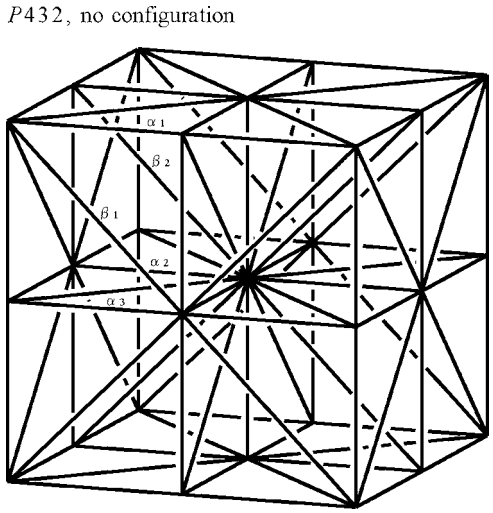

FIGURE 32. $P432$, G-orbits, no configuration.

3.4.4. $P6_322$

$\tilde{\mathcal{L}}$ consists of two G-orbits. We name α the orbit on the top level and β the orbit on the second level. We need both orbits to generate G. See Fig. 31.

C30: $\mathcal{L} = \tilde{\mathcal{L}} = \alpha \cup \beta$

3.5. Cubic system O

3.5.1. $P432$

$\tilde{\mathcal{L}}$ consists of five G-orbits. We name $\alpha_1, \alpha_2, \alpha_3$ the orbits parallel to x-axis and β_1, β_2 the orbits parallel to 110-axis. There exists a vertex of type O. No orbits in $\mathcal{L}$ would meet those vertices. So there is no possible configuration. See Fig. 32.

3.5.2. $P4_232$

$\tilde{\mathcal{L}}$ consists of five G-orbits. We name $\alpha_1, \alpha_2, \alpha_3$ the orbits parallel to x-axis and β_1, β_2 the orbits parallel to 110-axis. The intersecting triads at vertices of type D_2 are:

$$(\alpha_1, \alpha_1, \alpha_1), \quad (\alpha_1, \alpha_2, \alpha_3), \quad (\alpha_2, \beta_1, \beta_2), \quad (\alpha_3, \beta_1, \beta_2)\,.$$

Therefore, $\mathcal{L}$ does not contain α_1. We get two possible configurations. See Figs. 33, 34.

C31: $\mathcal{L} = \alpha_2 \cup \alpha_3 \cup \beta_1$
C32: $\mathcal{L} = \beta_1 \cup \beta_2$

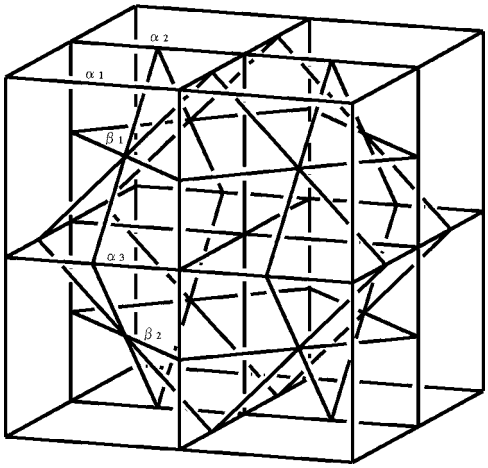

FIGURE 33. $P4_232$, G-orbits.

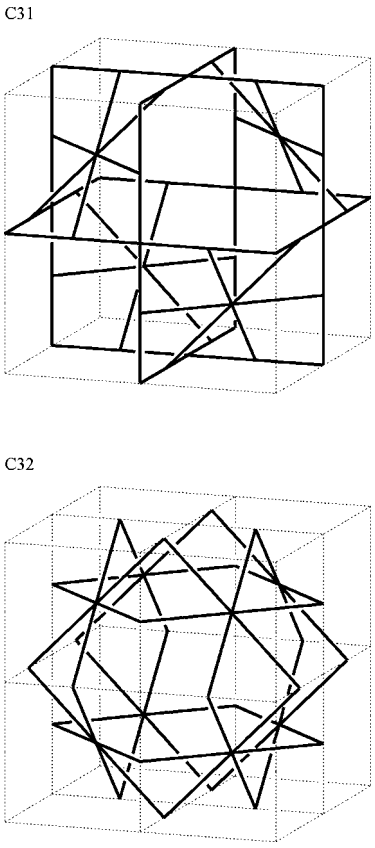

FIGURE 34. Configurations: C31, C32.

3.5.3. $F432$

$\tilde{\mathcal{L}}$ consists of four G-orbits. We name α_1, α_2 the orbits parallel to x-axis and β_1, β_2 the orbits parallel to 110-axis. There exists a vertex of type O. No orbits in $\mathcal{L}$ would meet those vertices. So there is no possible configuration. See Fig. 35.

3.5.4. $F4_132$

$\tilde{\mathcal{L}}$ consists of two G-orbits. We name α the orbit parallel to x-axis and β the orbit parallel to 110-axis. There exists a vertex of type D_2. The intersecting triad is (α, α, α). So α is not in $\mathcal{L}$. The orbit β generates G. So we have a possible configuration. See Fig. 36.

C33: $\mathcal{L} = \beta$

3.5.5. $I432$

$\tilde{\mathcal{L}}$ consists of four G-orbits. We name α_1, α_2 the orbits parallel to x-axis and β_1, β_2

$F4_132$

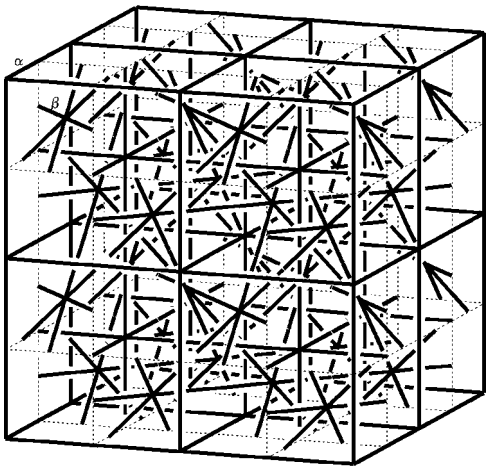

$F432$, no configuration

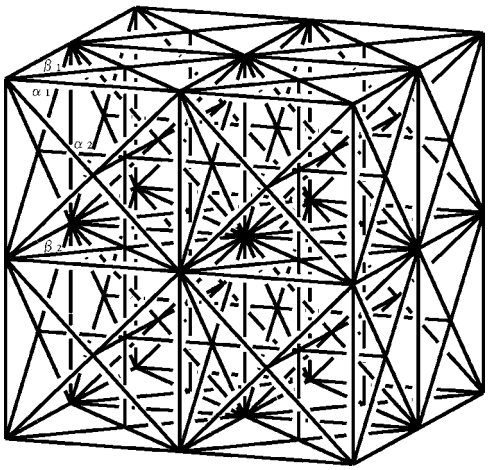

FIGURE 35. $F432$, G-orbits, no configuration.

C33

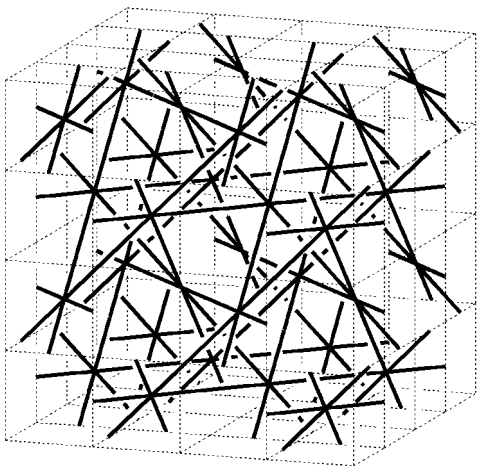

FIGURE 36. $F4_132$, G-orbits, configuration: C33.

the orbits parallel to 110-axis. There exists a vertex of type O. The orbits that do not meet those vertices are α_2 and β_2. But these two orbits intersect at vertices of type D_2, where the intersecting triad is $(\alpha_2, \beta_2, \beta_2)$. So only β_2 could be contained in $\mathcal{L}$. But this does not generate G. There is no possible configuration. See Fig. 37.

$I432$, no configuration

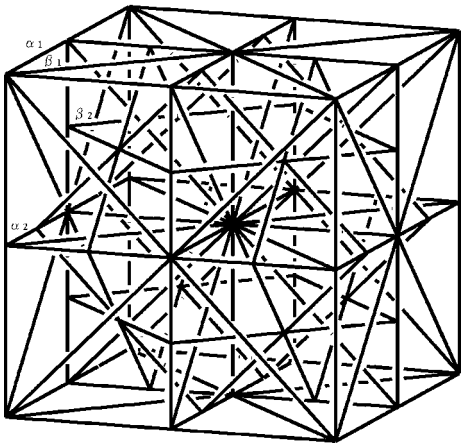

FIGURE 37. $I432$, G-orbits, no configuration.

$P4_332$, C34

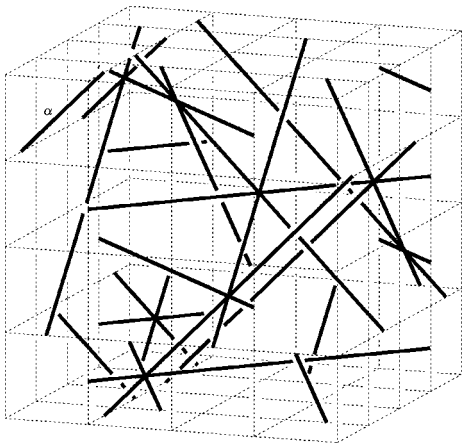

FIGURE 38. $P4_332$, G-orbit, configuration: C34.

3.5.6. $P4_332$

$\tilde{\mathcal{L}}$ consists of only one G-orbit. All vertices are of type D_3. So $\mathcal{L} = \tilde{\mathcal{L}}$. See Fig. 38.

C34: $\mathcal{L} = \tilde{\mathcal{L}} = \alpha$

3.5.7. $I4_132$

$\tilde{\mathcal{L}}$ consists of three G-orbits. We name α the orbit parallel to x-axis and β_1, β_2 the orbits parallel to 110-axis. There exists a vertex of type D_2. The intersecting triad is $(\alpha, \beta_1, \beta_2)$. By the symmetry, we have two possible configuration. See Figs. 39, 40.

C35: $\mathcal{L} = \alpha \cup \beta_1$
C36: $\mathcal{L} = \beta_1 \cup \beta_2$

4. Spatial polygons that could possibly generate triply periodic minimal surfaces

We call a finite spatial graph Γ to be a **spatial polygon** if it represents a simple closed curve. We assume that Γ generates a triply periodic minimal surface S. Then Γ defines a configuration $\mathcal{L}$ and the symmetries of $\mathcal{L}$ generates a transformation group G. Also, we denote $\tilde{\mathcal{L}}$ the set of all the axes of the symmetries in G.

Consider Γ as a set of edges. Then the G-orbits of the edges of Γ cover $\mathcal{L}$. The lines in $\mathcal{L}$ are covered by these edges. Thus we have a structure of graph over $\mathcal{L}$, consisting of these edges and vertices. These vertices are the same as in the previous section.

We denote the set of edges of $\mathcal{L}$ by $E(\mathcal{L})$. Then Γ meets every G-orbit in $E(\mathcal{L})$. Let G_Γ be the stationary group of Γ:

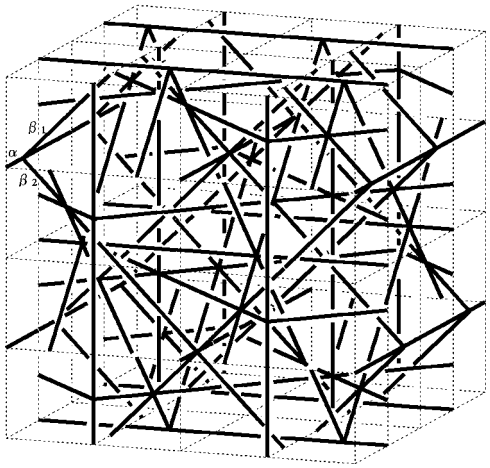

FIGURE 39. $I4_132$, G-orbits.

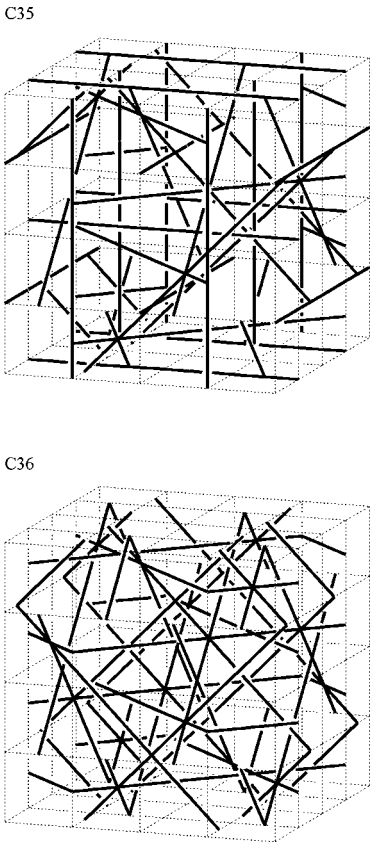

FIGURE 40. Configurations: C35, C36.

$$G_\Gamma = \{g \in G \mid g\Gamma = \Gamma\}.$$

Then G_Γ acts on Γ freely. Since this action preserves the cyclic structure of Γ, G_Γ is a cyclic group. We call its order as the **degree** of Γ. It is an order of an element of G. Let d be the degree of Γ and let k be the number of G-orbits in $E(\mathcal{L})$, then Γ is a dk-gon.

Γ bounds a compact domain S_Γ of S and S_Γ and $\mathcal{L}$ intersect only at Γ. Therefore, for any line l in $\mathcal{L}$ the linking number link(l, Γ) is zero. That is, no line in $\mathcal{L}$ could pass through or penetrate Γ. Then, also, the axis of G_Γ is not contained in $\mathcal{L}$.

The group G is generated by the symmetries of edges of Γ. Then, the configuration $\mathcal{L}$ is connected. In the previous section we have classified the configurations. In this section, we are only interested in connected configurations. They are fourteen types:

C2, C3, C4, C16, C17, C27, C28, C29, C31, C32, C33, C34, C35, C36

Here we mention roughly the process to find Γ from $\mathcal{L}$. Let k be the number of the G-orbits in $E(\mathcal{L})$. Choose initial edge e_1 arbitrarily. Find edge-paths $e_1, e_2, \cdots, e_k, e_{k+1}$

satisfying turn-to-the-first-corner principle. That is, at the vertex v_i joining e_i and e_{i+1}, these two are the nearest among branches at v_i. For each e_i, there are exactly two possible e_{i+1}'s, and they are in the same G-orbits. Check that $e_1, e_2, \cdots, e_k$ belong to all different G-orbits and e_1 and e_{k+1} belong to the same G-orbit. If $e_1 = e_{k+1}$ then we have a possible polygon of degree 1, or else we try to find a rotational symmetry ρ with $\rho e_1 = e_{k+1}$, which would generate G_Γ.

4.1. Orthorhombic system D_2

4.1.1. $P222$, Configuration C2

$E(\mathcal{L})$ is partitioned into six G-orbits. There are one generating polygon P1 of degree 1 and another generating polygon P2 of degree 2. See Fig. 42.

4.1.2. $P222$, Configuration C3

$E(\mathcal{L})$ is partitioned into six G-orbits. There is only one generating polygon P3 of degree 1. See Fig. 43.

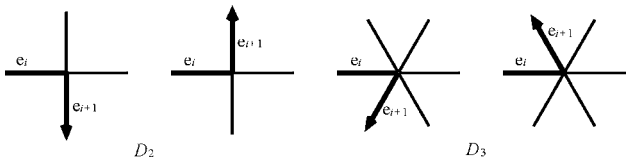

FIGURE 41. Turn-to-the-first-corner principle.

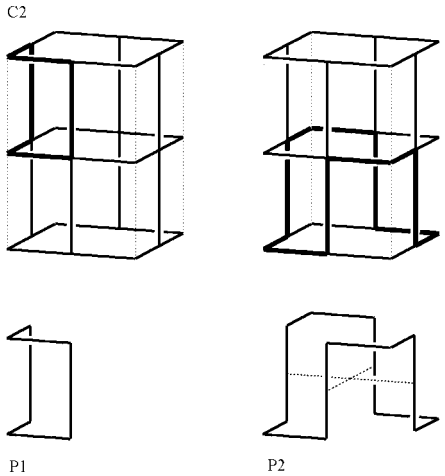

FIGURE 42. $P222$, C2, generating polygons: P1, P2.

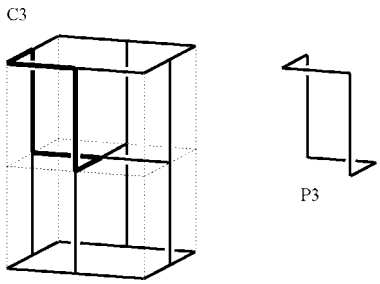

FIGURE 43. $P222$, C3, generating polygon: P3.

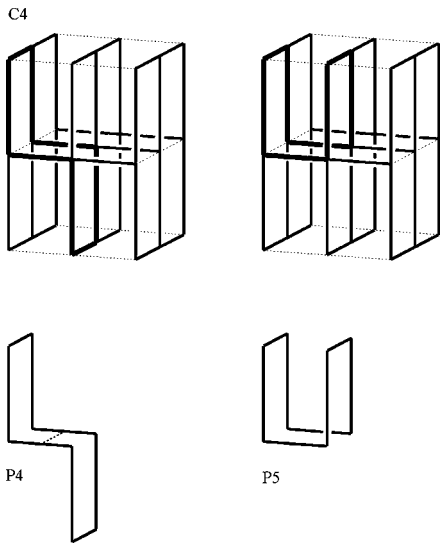

FIGURE 44. $P222$, C4, generating polygons: P4, P5.

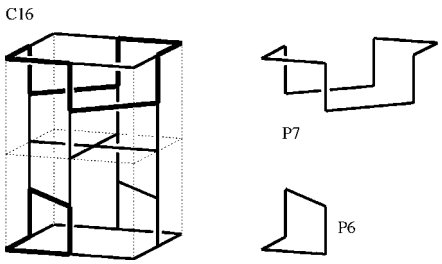

FIGURE 45. $P4_222$, C16, generating polygons: P6, P7.

4.1.3. $P222$, **Configuration** C4

$E(\mathcal{L})$ is partitioned into eight G-orbits. There are two generating polygons P4, P5 of degree 1. There is no generating polygon of degree 2. See Fig. 44.

4.2. Tetragonal system D_4

4.2.1. $P4_222$, **Configuration** C16

$E(\mathcal{L})$ is partitioned into five G-orbits. There are one generating polygon P6 of degree 1 and another generating polygon P7 of degree 2. See Fig. 45.

4.2.2. $P4_222$, **Configuration** C17

$E(\mathcal{L})$ is partitioned into six G-orbits. There are one generating polygon P8 of degree 1, and another generating polygon P9 of degree 2. See Fig. 46.

4.3. Hexagonal system D_6

4.3.1. $P6_222$, **Configuration** C27

$E(\mathcal{L})$ is partitioned into four G-orbits. Two are vertical and the other two are horizontal. One vertical edge is three times longer than the other. Therefore there is no generating polygon of degree 1. There are two polygons of degree 2. One is the generating polygon P10, but the other polygon has a penetrating line in $\mathcal{L}$. See Fig. 47.

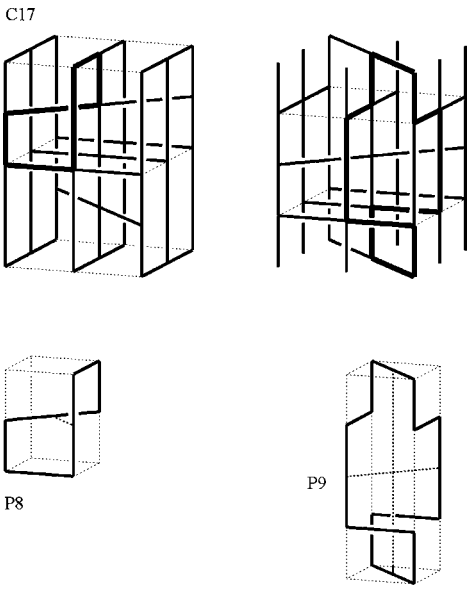

FIGURE 46. $P4_222$, C17, generating polygons: P8, P9.

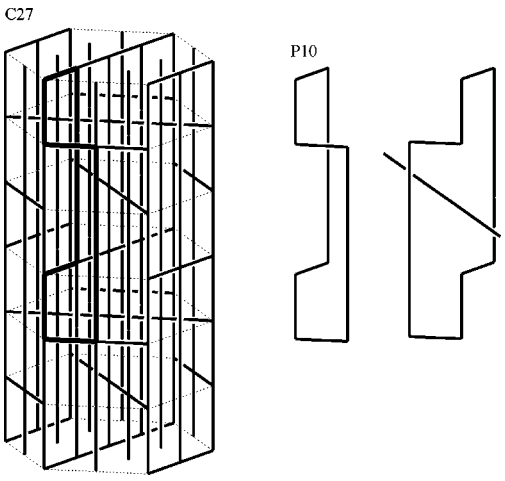

FIGURE 47. $P6_222$, C27, generating polygon: P10.

4.3.2. $P6_222$, **Configuration** C28

$E(\mathcal{L})$ is partitioned into four G-orbits. There is no generating polygon of degree 1. There are two polygons of degree 2. But both have penetrating lines in $\mathcal{L}$. Hence there is no generating polygon. See Fig. 48.

4.3.3. $P6_222$, **Configuration** C29

$E(\mathcal{L})$ is partitioned into four G-orbits. There is no generating polygon of degree 1. There are two polygons of degree 2. One is the generating polygon P11, but the other polygon has a penetrating line in $\mathcal{L}$. See Fig. 49.

4.4. Cubic system O

4.4.1. $P4_232$, **Configuration** C31

$E(\mathcal{L})$ is partitioned into four G-orbits. Two contain edges parallel to x-axis and the other two contain edges parallel to 110-axis. For the latter case, one line is decomposed into two G-orbits as: $\ldots aabbaabb\ldots$. There is one generating polygon P12 of degree 1 and another generating polygon P13 of degree 3. There is no generating polygon of degree 2. See Fig. 50.

4.4.2. $P4_232$, **Configuration** C32

$E(\mathcal{L})$ is partitioned into four G-orbits. All edges are congruent and all G-orbits contain edges parallel to 110-axis. Each line is decomposed into two G-orbits as: $\ldots aabbaabb\ldots$. There is one generating polygon P14 of degree 1 and another generating polygon P15 of

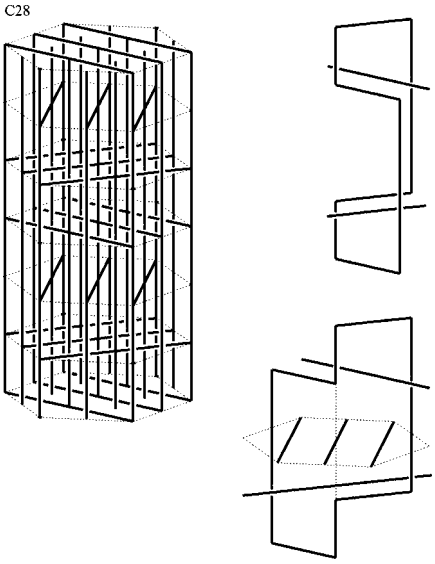

FIGURE 48. $P6_222$, C28, no generating polygon.

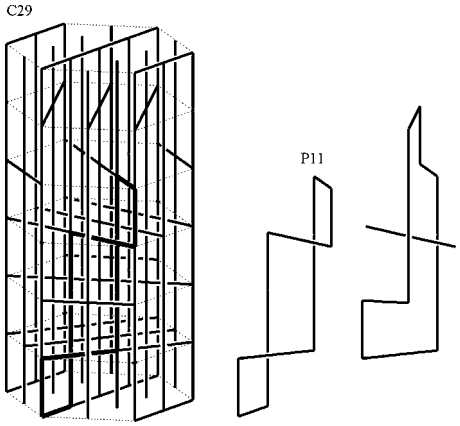

FIGURE 49. $P6_222$, C29, generating polygon: P11.

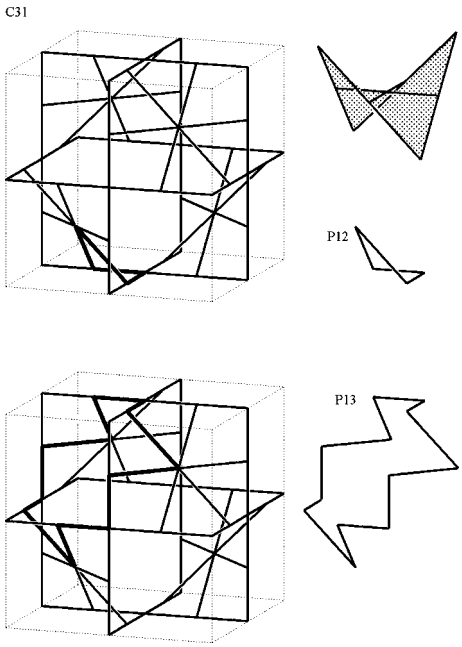

FIGURE 50. $P4_232$, C31, generating polygons: P12, P13.

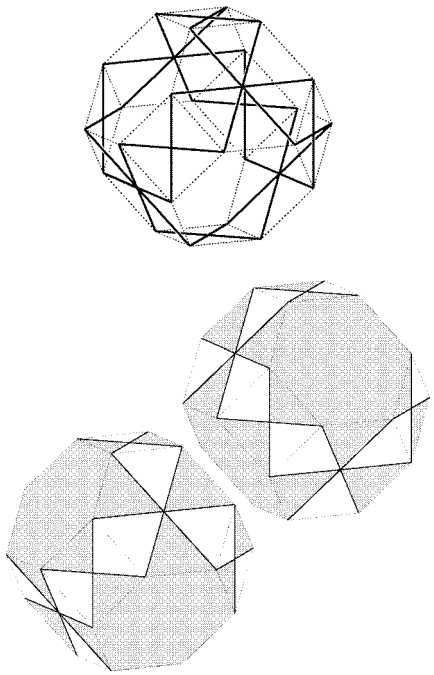

FIGURE 51. $P4_232$, C31, P13, embedded triply periodic minimal surface.

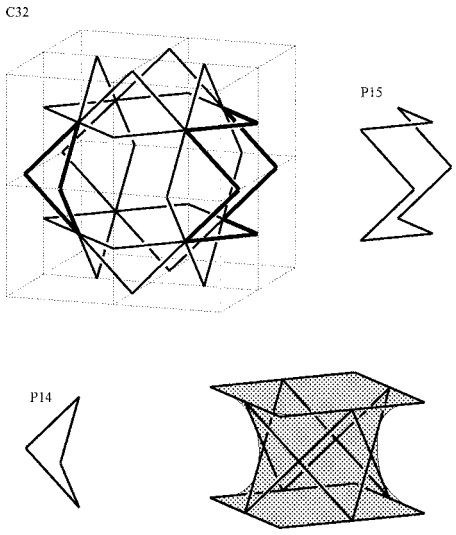

FIGURE 52. $P4_232$, C32, generating polygons: P14, P15.

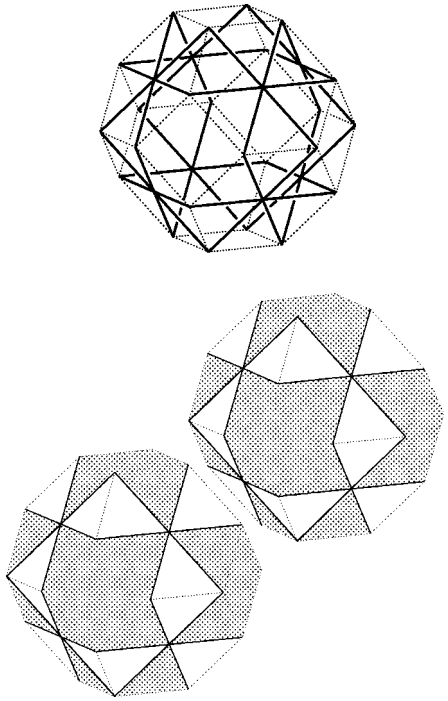

FIGURE 53. $P4_232$, C32, P15, embedded triply periodic minimal surface.

degree 2. There is no generating polygon of degree 3. See Fig. 52.

4.4.3. $F4_132$, **Configuration** C33

$E(\mathcal{L})$ is partitioned into two G-orbits. All edges are congruent and all G-orbits contain edges parallel to 110-axis. Each line is decomposed into two orbits as: $\ldots ababab \ldots$. There are one generating polygon P16 of degree 2 and another generating polygon P17 of degree 3. There is no generating polygon of degree 1. See Fig. 54.

4.4.4. $P4_332$, **Configuration** C34

$E(\mathcal{L})$ is partitioned into two G-orbits. One edge is three times longer than the other. All G-orbits contain edges parallel to 110-axis. Each line is decomposed into two orbits of different length as: $\ldots slslsl \ldots$. There is no generating polygon of degree 1, neither of degree 2 or 3.

4.4.5. $I4_132$, **Configuration** C35

$E(\mathcal{L})$ is partitioned into three G-orbits. One contains an edge parallel to x-axis and the other two contain edges parallel to 110-axis. For the latter orbits, one is three times longer than the other. A line parallel to 110-axis is decomposed into two orbits as: $\ldots ssllssll \ldots$.

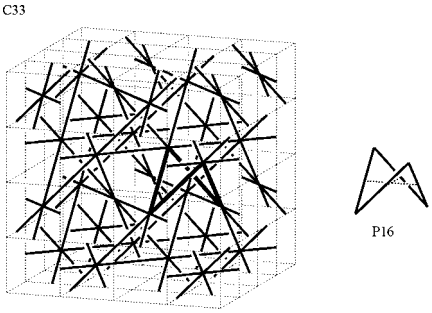

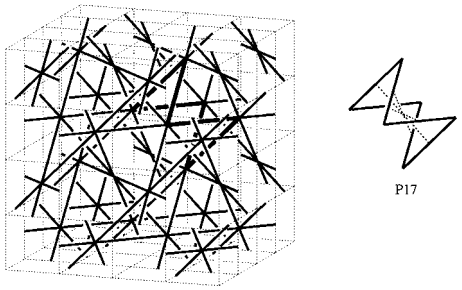

FIGURE 54. $F4_132$, C33, generating polygons: P16, P17.

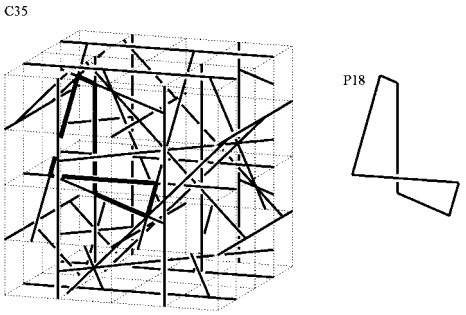

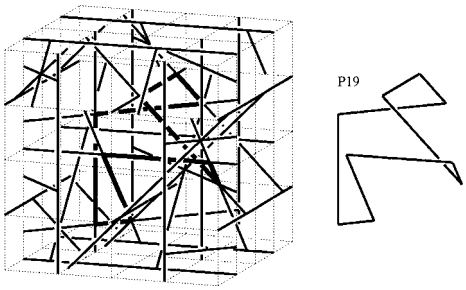

FIGURE 55. $I4_132$, C35, generating polygons: P18, P19.

There is no generating polygon of degree 1. There is only one generating polygon P18 of degree 2. Also, there is only one generating polygon P19 of degree 3. See Fig. 55.

4.4.6. $I4_132$, **Configuration** C36

$E(\mathcal{L})$ is partitioned into four G-orbits. Two are long and the other two are short. The longer edges are congruent and the shorter edges are congruent too. All G-orbits contain edges parallel to 110-axis. Each line is decomposed into two orbits as: $\ldots ssllssll \ldots$. There is no generating polygon of degree 1. There are three polygons of degree 2. But the two are congruent each other and they have penetrating lines in $\mathcal{L}$. So, there is only one generating polygon P20 of degree 2. Also, there are two polygons of degree 3. One has penetrating lines in $\mathcal{L}$. There is also only one generating polygon P21 of degree 3. See Figs. 56, 57.

5. Spanning minimal surfaces

Here, we list the known results concerning to the triply periodic minimal surfaces generated by our spatial polygons.

5.1. Nitsche Polygons. A spatial polygon Γ is called to be a Nitsche polygon, if the following condition holds:

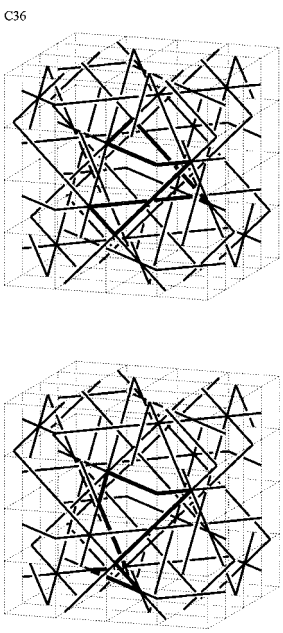

FIGURE 56. $I4_132$, C36, generating polygon: P20.

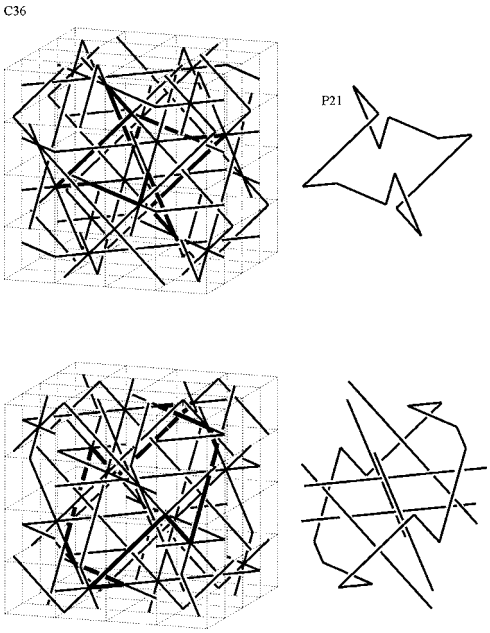

FIGURE 57. $I4_132$, C36, generating polygon: P21.

i) Γ projects to a convex polygon in a plane, and

ii) let $\pi : \Gamma \to \pi(\Gamma)$ be the projection, then $\pi^{-1}(x)$ is either a point or a line segment.

Let Γ be a Nitsche polygon, then there is a Plateau solution S_Γ for Γ. S_Γ is homeomorphic to a disk. S_Γ is unique in the sense that if there exist a compact minimal surface of any genus bounded by Γ then it must coincide with S_Γ.

For our spatial polygons, P1–P8 and P12–P17 are Nitsche polygons. So, they bound unique Plateau disks S_Γ's.

5.2. Orthorhombic system D_2. The polygons belonging to the orthorhombic system are P1–P5. All of them are Nitsche polygons.

- P1 is known to generate the CLP-surface [5]. See Fig. 42.
- P2 has line symmetries whose axes pass the pairs of the midpoints of the horizontal edges and P2 decomposes into four P3-type polygons. Since the Plateau disk is unique, the spanning surface for P2 is the same as the spanning surface for P3. See Figs. 42, 43.
- P3 is known to generate the least symmetric Schwarz D-surface [5].
- P4 has a line symmetry whose axis passes the midpoints of the horizontal edges and P4 decomposes into two P1-type polygons. So, the spanning surface for P4 is the same as the spanning surface for P1. See Fig. 44.

- P5 generate embedded triply periodic minimal surfaces treated in [3].

5.3. Tetragonal system D_4. The polygons belonging to the tetragonal system are P6–P9. Except P9, all of them are Nitsche polygons.

- P6 is known to generate the Gergonne surface [9], which is also a less symmetric Schwarz D-surface. See Fig. 45.
- P7 generate a triply periodic minimal surface.
- P8 has a line symmetry whose axis passes the midpoint of the long vertical edge and the midpoint of the long horizontal edge and P8 decomposes into two P6-type polygons. So, the spanning surface for P8 is the same as the spanning surface for P6. See Fig. 46.
- P9 has two line symmetries whose axes are z-axis and 110-axis. If the spanning surface S_Γ inherits this symmetry, then it contains these axes and P9 decomposes into four P8-type polygons. So, P9 does generate a triply periodic minimal surface which is the same surface as the spanning surface for P6. But there remains a small possibility that another S_Γ, with genii, does not inherit the symmetry.

5.4. Hexagonal system D_6. The polygons belonging to the hexagonal system are P10–P11. These two are not Nitsche polygons.

- P10 generates an embedded triply periodic minimal surface shown in [6]. See Fig. 47.
- The existence of the spanning surface for P11 is not known.

5.5. Cubic system O. The polygons belonging to the cubic system are P12–P21. Among them, P12–P17 are Nitsche polygons.

- P12 bounds one quarter of the Riemann-Schwarz' diamond surface (or Schwarz D-surface) [1, 5]. See Fig. 50.
- For P13, we can embed four copies of the Plateau disk S_Γ in the truncated octahedron. By the tessellation, we can get an embedded triply periodic minimal surface. It is known as the C(D)-surface [1, 5]. See Fig. 51.
- P14 bounds the conjugate of the Riemann-Schwarz' diamond surface (or the Schwarz P-surface) [1, 5]. Twelve copies of this surface together form a catenoid-like minimal surface between two parallel squares. See Fig. 52.
- For P15, we can embed six copies of the Plateau disk S_Γ in the truncated octahedron. By the tessellation, we can get an embedded triply periodic minimal surface, known as the C(P)-surface [1, 5]. See Fig. 53.
- P16 has two line symmetries whose axes pass the pairs of the midpoints of the edges and it decomposes into four P12-type polygons. So, the spanning surface for P16 is the Schwarz D-surface. See Fig. 54.

- P17 has three line symmetries whose axes pass the pairs of the midpoints of the edges and it decomposes into six P14-type polygons. So, the spanning surface for P17 is the Schwarz P-surface.
- The existence of the spanning surfaces for P18–P21 is not knowm.

References

[1] A. H. SCHOEN, Infinite periodic minimal surfaces without self-intersections, NASA Technical Note No. TN D-5541 (1970).

[2] T. HAHN (ed.), *International tables for crystallography, vol. A*, D. Reidel Pub. Co. (1987).

[3] H. KARCHER, Embedded minimal surfaces derived from Scherk's examples, Manuscripta Math. **62** (1988), 83–114.

[4] J. C. C. NITSCHE, *Lectures on minimal surfaces, vol. 1*, Cambridge University Press (1989).

[5] H. KARCHER, The triply periodic minimal surfaces of Alan Schoen and their constant mean curvature companions, Manuscripta Math. **64** (1989), 291–357.

[6] D. HOFFMAN, Natural minimal surfaces via theory and computation (video), Science Television Production (1990).

[7] B. IVERSEN, *Lectures on crystallographic groups*, Aarhus Universitet (1990).

[8] E. KOCH and W. FISCHER, A crystallographic approach to 3-periodic minimal surfaces, Statistical thermodynamics and differential geometry of microstructural materials (Minneapolis, MN, 1991) 15–48, IMA Vol. Math. Appl. **51** (1993), Springer.

[9] H. KARCHER and K. POLTHIER, Construction of triply periodic minimal surfaces, Phil. Trans. R. Soc. Lond. A **354** (1996), 2077–2104.

Present Address:
DEPARTMENT OF MATHEMATICS, GAKUSHUIN UNIVERSITY,
MEJIRO, TOSHIMA-KU, TOKYO, 171–8588 JAPAN.